

## Emission Cross Sections for the $N_2$ Second Positive (0, 0) Transition for H, $H^+$ , He, and $He^+$ Impact\*

J. M. Hoffman, G. J. Lockwood, and G. H. Miller

*Sandia Laboratories, Albuquerque, New Mexico 87115*

(Received 23 August 1972)

Absolute emission cross sections for 3371-Å radiation resulting from  $C^3\Pi_u(v'=0) \rightarrow B^3\Pi_g(v''=0)$  transition in molecular nitrogen have been measured for H,  $H^+$ , He, and  $He^+$  projectiles. The energy range covered was from 10 to 100 keV for all projectiles except  $H^+$ , where the lower limit was 40 keV. Excitation of the  $C^3\Pi_u$  upper state requires a spin change, usually accomplished by interchange of electrons. Thus the cross section for  $H^+$  impact is very small ( $\lesssim 10^{-19}$  cm<sup>2</sup>) and could not be measured reliably below 40 keV at this time. Some emission cross sections are presented for incident helium atoms in the  $2^3S$  metastable state. Comparisons are made of  $He^+$  and H data, where the minimum excitation energy required is the same, and of  $He^+$  and He data, where the minimum excitation energies are quite different. Cross sections are also presented for emission of the  $N_2^+$  (3914-Å) band for protons in the 8–30 keV energy range, permitting comparison with the measurements of other investigators.

### I. INTRODUCTION

In this paper we report emission cross sections for 3371-Å radiation from the second positive system of  $N_2$  resulting from the incidence of certain projectiles on a gaseous nitrogen target. These projectiles were atoms of H and He as well as singly charged ions of He, all in the energy range from about 10 to 100 keV. Difficulties associated with measurement of the 3371-Å emission cross section for incident protons are discussed, and data are presented in the range from 40 to 100 keV. In addition, data are presented on  $N_2^+$  (3914-Å) radiation resulting from proton collisions with  $N_2$  in the energy range from 8 to 30 keV.

The second positive system of  $N_2$  plays an important part in upper atmospheric phenomena. The excitation of the initial state ( $C^3\Pi$ , excitation energy = 11 eV) involves a spin change from the  $^1\Sigma$  ground state. This is generally thought to take place by electron interchange. Thus one might expect that  $H^+$  ions should have at best a small cross section. Measurements<sup>1,2</sup> indicate that this is indeed the case. Although these two sets of measurements cover different energy ranges and appear to be in disagreement, it is clear that the cross section is small.

In excitation of the  $C^3\Pi$  state by either H or  $He^+$ , the electron may be interchanged without excitation of the projectile. Only the 11-eV excitation for the  $N_2$  is required. Differences in the cross sections for the two cases then result from the difference in the binding energy of the electron in the projectile (13.6 eV for H, 54.4 eV for  $He^+$ ), the net charge of the projectile, and the projectile mass. Although the present investigation does not determine which of these properties are important, it serves to determine whether a difference in cross sections

exists.

In the case of He projectiles the situation is different. If the He atom is in the ground state ( $^1S$ ), spin conservation requires that it change to a triplet state for excitation of  $N_2$  to the  $C^3\Pi$  state. This, however, requires an additional 19.8 eV for excitation of the He; thus the total energy is about three times that required for either H or  $He^+$ . One would expect that the cross sections for He would be less at low velocities and peak at a higher velocity than those for  $He^+$ .

A very interesting case should be that for which the projectile has metastable excitation and where the excitation energy can be made available in the electron interchange. For example, the H(2s),  $He^+(2s)$ , and He( $2^3S$ ) states all qualify. The hydrogen case should be particularly important since the 2s-state excitation (10.2 eV) is close to that required for excitation of the  $C^3\Pi$  state. While we have not examined this case, we have been able to make a crude determination of the cross section at several energies for the He ( $2^3S$ ) projectile.

Making absolute emission-cross-section measurements requires that the calibration be accomplished through the use of some standard radiation source. In order to compare calibrations between various laboratories, it is useful to measure some common cross section. The  $N_2^+$  (3914-Å) emission cross sections resulting from  $H^+$  projectiles have been measured by a number of investigators.<sup>1-8</sup> The lack of agreement among these investigators indicates the severity of the problem of making absolute measurements. By presenting our 3914-Å results we thus provide not only absolute measurements but also a means of comparison with other investigators.

One final set of measurements results as a by-product of the method employed. In general, with

the second positive system, there are relatively large effects present which are second order with pressure. Low-energy electrons ( $\sim 15$  eV) have a large cross section<sup>9</sup> for excitation of the C<sup>3</sup>Π level; thus secondary collisions of ionization electrons have an important contribution to the signal. Since the technique involves measurement of the signal as a function of pressure, the second-order coefficient is determined. Hence some information relative to second-order effects is obtained.

## II. APPARATUS AND PROCEDURES

Sandia Laboratories's 100- and 25-kV positive-ion accelerators used in this study delivered beams of magnetically analyzed ions having small energy spread ( $\Delta E < 50$  eV) to the experimental chambers. The energies were determined to 2% by measuring the terminal potential with a voltage divider and correcting for source potential. Similar experimental apparatus was used with both accelerators.

Accordingly, the following discussion pertains to both systems. In obtaining the absolute cross sections reported here, each experimental system was calibrated independently, and the absolute values of cross sections were found to be in very good agreement in the overlap energy range.

The ion beams from the accelerators entered the experimental apparatus, shown in Fig. 1, through aperture A and passed through apertures B, C, and D into the interaction region. The interaction was viewed at approximately 1 cm after aperture D. For excitation studies with H<sup>+</sup> and He<sup>+</sup>, the charge transfer cell between A and B was evacuated and the deflection plates between B and C were grounded. When hydrogen-atom excitation cross sections were measured, the charge-transfer cell between

A and B was filled with Kr at a pressure of approximately 7 mTorr and a voltage applied to the deflection plates sufficient to remove all residual protons. Krypton was used as the transfer gas, since the energy defect for transfer to the ground state of H is only 0.4 eV. It is expected that this should produce a relatively pure ground-state hydrogen beam. Also, the electric field used to remove the residual protons produced a calculated lifetime for the 2s state which was short compared to the time spent in the field. Therefore, the 2s state should have been quenched.<sup>10</sup> Variation of this field over a wide range (0.5–8 kV/cm) produced no observable differences in the cross section.

For helium-atom excitation cross sections, the charge-transfer cell between A and B was filled with either helium, hydrogen, or xenon. When helium gas at high pressure is used, the resulting atom beam contains less than 1% metastable helium atoms.<sup>11</sup> However, if the charge transfer takes place in hydrogen or xenon at low pressure, the atom beam thus formed contains from 5 to 25% metastable atoms, depending on the incident-ion energy. By application of the published fraction in the metastable state<sup>11</sup> when the beam was charge transferred in low-pressure hydrogen or xenon, the emission cross section for incident metastable helium atoms was deduced.

The interaction chamber was differentially pumped with aperture D (2.03 mm diam) determining the gas flow. The nitrogen was passed through a liquid-N<sub>2</sub> cold trap and the flow rate was controlled by a mechanical leak. The pressure range used was 0.4–6 mTorr, with the pressure being measured by a capacitance manometer. The temperature of the target chamber was 18 °C for all

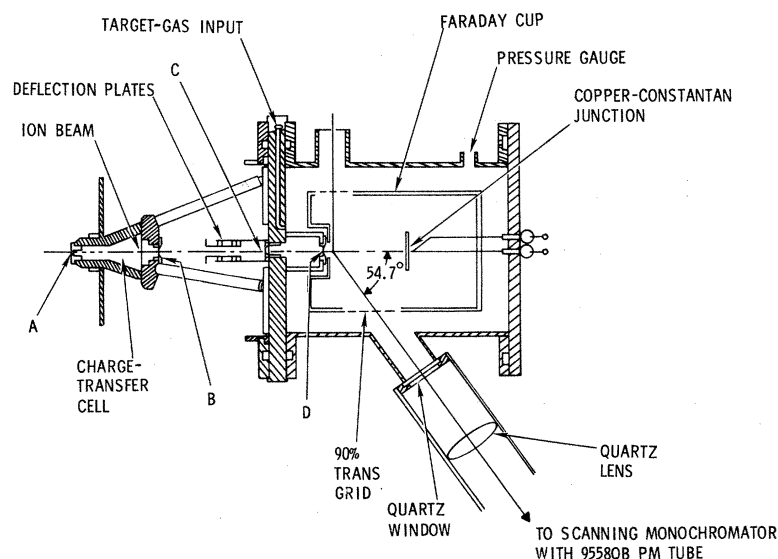


FIG. 1. Experimental apparatus.

measurements. Effusion of the gas through the aperture results in a target thickness somewhat greater than the geometrical value. Under the conditions employed, the effective gas target thickness was estimated to be 1.6 cm to the viewing region. However, because of the long flight path from the analyzing magnet to the interaction chamber, the ion beam did contain a small but unknown fraction of neutrals made by charge transfer.

The interaction region was surrounded by a Faraday cup which gave an accurate measure of the ion current when there was no gas in the interaction chamber. However, it could not be used to measure the atom beams under any condition, or to measure the ion beams when interaction gas was present because of processes which occurred in the entrance region of the interaction chamber. For these reasons a target-thermocouple combination was placed inside the Faraday cup and used for all particle current measurements. The thermocouple was calibrated against the Faraday cup signal when no interaction gas was added. It then provided an accurate measure of the fast-particle current entering the interaction region. The design of this system was such that heat was removed almost exclusively by conduction. Tests showed that radiation loss was small and that target gas pressure did not significantly affect the measurement.

The radiation passed through a quartz window into the optical system, which consisted of a quartz lens and a scanning monochromator having its slits normal to the beam axis. With the slit width used

here, resolution was approximately 21 Å. The axis of this system made an angle of 54.7° with the beam axis. Under this condition, intensity is independent of beam-radiation polarization. Instrument polarization was measured<sup>12</sup> and the resulting corrections to the cross sections were never more than 3%.

Data runs were obtained in the form of peak height of the spectral distribution as a function of pressure. Correlations were made between the integral over the spectral distribution and peak measurements for both incident ions and atoms as a function of pressure and energy. These measurements permitted the peak intensity to be used as a measure of the total number of photons associated with the selected radiations. Background signals were obtained from a spectral region adjacent to that of the desired transition and were subtracted from the desired signals. In every case the background was proportional to pressure and beam current.

To obtain absolute cross sections, the optical system was calibrated *in situ* by use of a quartz iodine-vapor standard lamp,<sup>12</sup> the calibration of which is traceable to the National Bureau of Standards. The light was scattered from a magnesium carbonate diffuse scatterer placed in the system at that part of the beam target interaction region which was viewed by the optical system. Corrections to the absolute calibration in the wavelength region from 3300 to 4000 Å necessitated by scattered light were found to be less than 3%.

### III. DATA

The signal resulting from incident ions is given approximately as a function of pressure by

$$i_s = C[i_1\sigma_{1e}Nlp + i_1\sigma_{10}Nlp(\sigma_{0e} - \sigma_{1e})Np + i_1N^2p^2I],$$

where  $i_s$  is signal current,  $C$  is the calibration constant which relates photons per unit path length to current from the detector, and  $i_1$  is incident ion current.  $\sigma_{1e}$ ,  $\sigma_{0e}$  are emission cross sections for ions and atoms, respectively,  $\sigma_{10}$  is the electron-capture cross section for ions,  $N$  is the number of molecules/cm<sup>3</sup> at 1 mTorr ( $3.32 \times 10^{13}$ /cm<sup>3</sup> at 18 °C), and  $p$  is the pressure in millitorr.  $l$  is the effective chamber depth in centimeters to the observation region and  $I$  is an integral over ionization cross section, electron energy and angle distributions, electron-induced emission cross section, and path in the chamber.

It can be observed that the normalized signal is of the form

$$i_s/i_1 = a_1p + a_2p^2.$$

A similar expression can be obtained for the signal resulting from incident neutral atoms by replacing 1 and 0 by 0 and 1, respectively. It is convenient to divide this equation by the pressure and

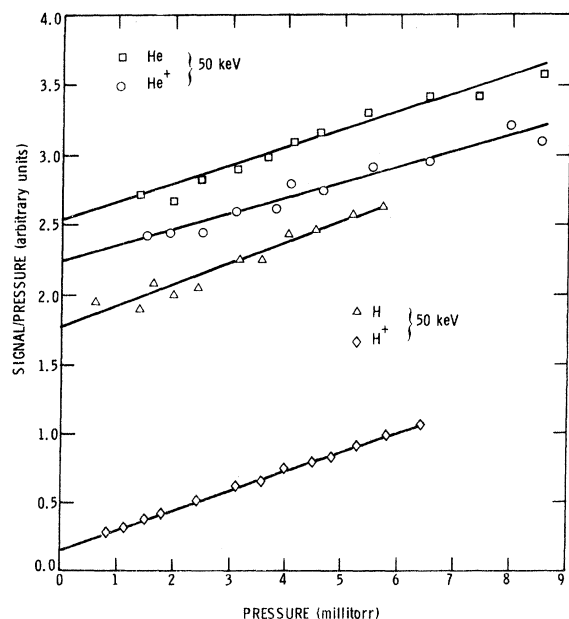


FIG. 2. Normalized signal-pressure ratio as a function of pressure for 3371-Å radiation resulting from impact of H<sup>+</sup>, H, He<sup>+</sup>, and He on N<sub>2</sub>.

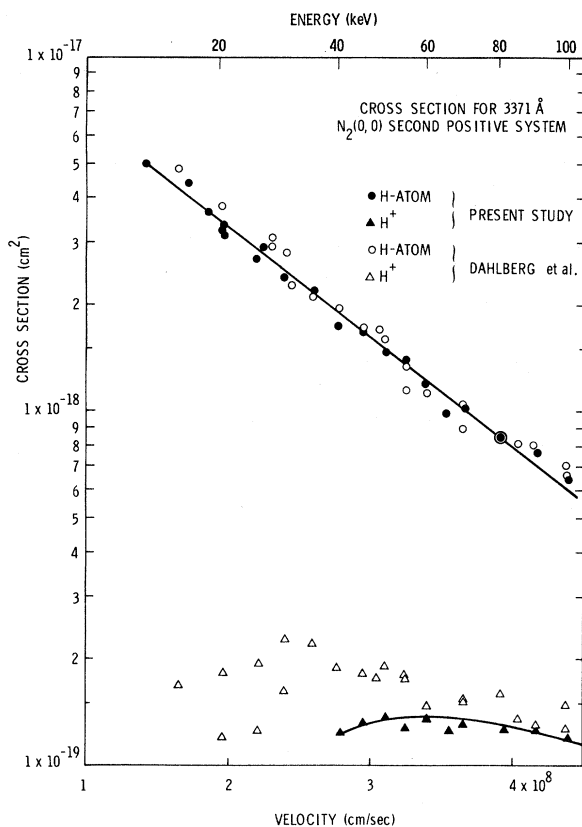


FIG. 3. Emission cross sections for the N<sub>2</sub> (3371-Å) transition as a function of velocity for incident H<sup>+</sup> and H atoms.

to plot the normalized signal-pressure ratio as a function of pressure. Typical curves of this type are shown in Fig. 2, where the solid lines are linear least-squares fits. The emission cross section can then be obtained from the intercept, while the magnitude of the second-order effects is related to the slope. The difficulty with this procedure is that it weights the lower-pressure points more heavily, and these should inherently be subject to greater percentage error. Attempts to weight the higher-pressure data more heavily led to substantially greater scatter of points in the cross-section-vs-energy curve. We believe that there are pressure effects taking place in the region between the magnet and the reaction chamber which depend on factors in addition to reaction-chamber pressure and which are more important at high pressure. As a result, the cross sections which are presented were obtained from the least-squares linear fit of normalized signal-pressure ratio as a function of pressure.

Cross sections are shown in Fig. 3 for incident H<sup>+</sup> and H atoms and in Fig. 4 for He<sup>+</sup> and He atoms. These values are also tabulated in Tables I and II.

As stated previously, we have measured the N<sub>2</sub><sup>+</sup>

(3914-Å) emission cross section for H<sup>+</sup> projectiles in order that our results can be compared with other measurements and hence allow a cross comparison of our calibration techniques with those used in other laboratories. Results of these measurements in the energy range from 8 to 30 keV are shown in Fig. 5. Also shown are the results of other investigations where absolute calibrations were made.

#### IV. DISCUSSION AND CONCLUSIONS

Before considering specific features of the 3371-Å results, some qualitative statements should be made. In general, we expect electron interchange between the projectile and the N<sub>2</sub> target to provide the mechanism for the spin change. While the adiabatic criterion is not expected to provide quantitative information, we expect that it is qualitatively valid. By this we mean that we expect that

TABLE I. First-order emission cross section for the production of 3371-Å radiation in N<sub>2</sub> produced by protons and H atoms. Units of cross section are 10<sup>-19</sup> cm<sup>2</sup>/molecule; units of velocity are 10<sup>8</sup> cm/sec; units of energy are keV; estimated experimental uncertainty in cross section is 15% for H atoms and 20% for H<sup>+</sup>.

| Energy  | Velocity | Cross section |
|---------|----------|---------------|
| Protons |          |               |
| 40.0    | 2.78     | 1.23          |
| 45.0    | 2.95     | 1.32          |
| 50.1    | 3.11     | 1.38          |
| 54.9    | 3.25     | 1.27          |
| 60.0    | 3.40     | 1.35          |
| 65.8    | 3.56     | 1.24          |
| 69.4    | 3.66     | 1.30          |
| 81.4    | 3.96     | 1.26          |
| 90.3    | 4.17     | 1.27          |
| 100.1   | 4.39     | 1.21          |
| H atoms |          |               |
| 10.4    | 1.42     | 49.8          |
| 15.3    | 1.72     | 44.0          |
| 18.0    | 1.86     | 36.0          |
| 19.9    | 1.96     | 32.1          |
| 20.0    | 1.97     | 31.0          |
| 20.0    | 1.97     | 33.0          |
| 25.0    | 2.20     | 27.0          |
| 26.0    | 2.24     | 28.8          |
| 30.1    | 2.41     | 23.7          |
| 34.7    | 2.59     | 22.0          |
| 39.9    | 2.77     | 17.4          |
| 45.0    | 2.95     | 16.7          |
| 50.5    | 3.12     | 14.7          |
| 54.6    | 3.24     | 14.0          |
| 59.1    | 3.38     | 11.9          |
| 64.5    | 3.53     | 9.89          |
| 69.7    | 3.67     | 10.1          |
| 80.1    | 3.93     | 8.51          |
| 90.0    | 4.17     | 7.66          |
| 100.1   | 4.39     | 6.47          |

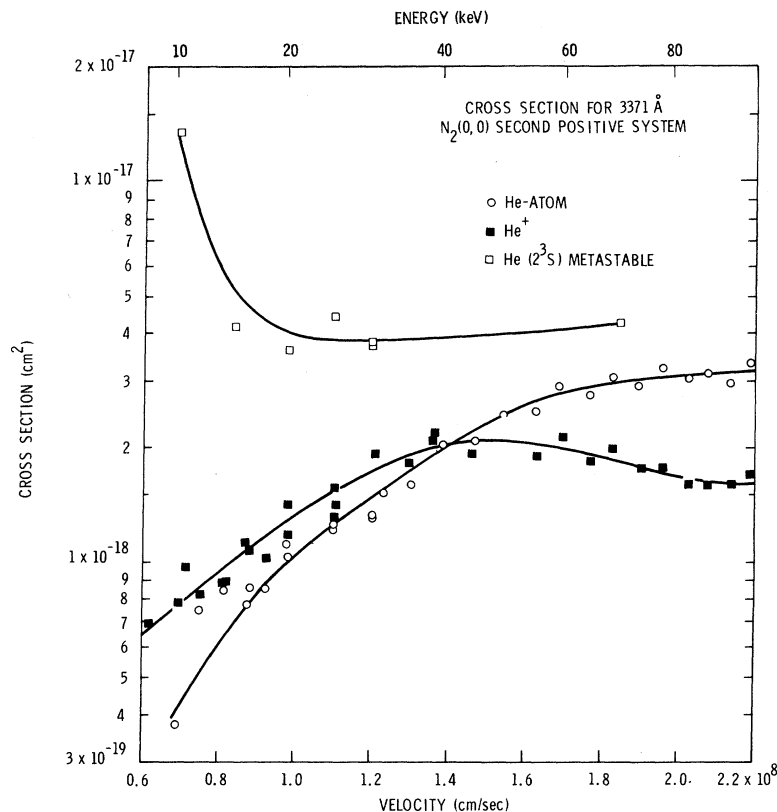


FIG. 4. Emission cross sections for the  $N_2$  (3371-Å) transition as a function of velocity for incident  $He^+$  and He atoms.

the cross section will have at least one maximum, and that the projectile velocity associated with such a maximum will be related to the  $\Delta E$  involved. The  $\Delta E$  represents the change in potential energy occurring in the collision. The magnitude of the cross section at any velocity is expected to depend on other factors as well as  $\Delta E$ . One of these is the radius of the orbit associated with the electron (of the projectile) participating in the interchange. The number of equivalent electrons in the projectile is an additional factor. In some cases the projectile mass may be important. This is not thought to be the case here. It has been found,<sup>1</sup> for example, that deuterons have about the same 3371-Å emission cross section as protons of the same velocity. Finally, the net charge of the projectile may influence the result.

The  $He^+$  and He data for the 3371-Å radiation can be understood on at least a qualitative basis. The velocities at which the maximum cross sections occur are consistent with the values of  $\Delta E$ . In the case of  $He^+$  ( $\Delta E = 11$  eV) the maximum is at about  $1.5 \times 10^8$  cm/sec, whereas for He ( $\Delta E = 31$  eV) the curve is still increasing at the maximum velocity which we can attain. It is interesting that He has a greater cross section than  $He^+$  for velocity greater than  $1.5 \times 10^8$  cm/sec. The effect of the larger  $\Delta E$  for He has apparently been overcome by the

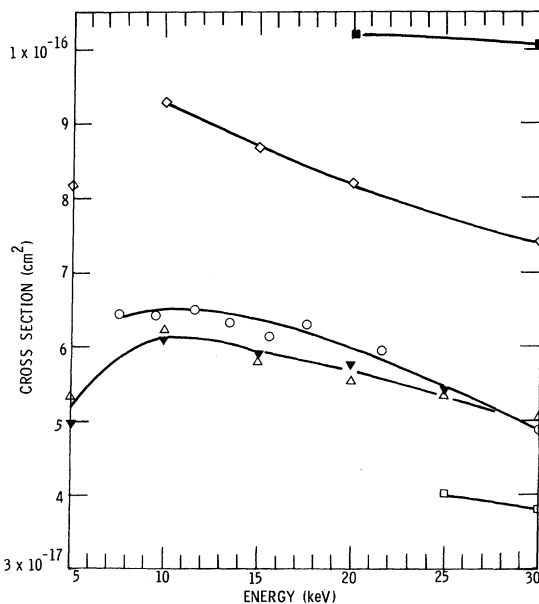


FIG. 5. Absolute emission cross sections for the  $N_2^+$  (3914-Å) transition resulting from proton impact on  $N_2$ , showing comparison of present results with other data. The stated errors for the data shown are ■ Gardiner *et al.* (Ref. 6) 25%; ◇ Philpot and Hughes (Ref. 3) 40%; △, Deheer and Aarts (Ref. 7) 15%; ▼ Sheridan *et al.* (Ref. 8) 20–25%; □, Dufay *et al.* (Ref. 4) 50%; and ○, present study 15%.

TABLE II. First-order emission cross section for the production of 3371-Å radiation in N<sub>2</sub> produced by He<sup>+</sup>, He atoms, and He metastable atoms. Units of cross section are 10<sup>-18</sup> cm<sup>2</sup>/molecule; units of velocity are 10<sup>8</sup> cm/sec; units of energy are keV; estimated experimental uncertainty in cross section is 15% for He<sup>+</sup> and He atoms (ground state) and 50% for He atoms (metastable).

| Energy | Velocity        | Cross section |
|--------|-----------------|---------------|
|        | He <sup>+</sup> |               |
| 8.0    | 0.61            | 0.69          |
| 10.0   | 0.69            | 0.74          |
| 10.6   | 0.72            | 0.97          |
| 12.0   | 0.75            | 0.83          |
| 14.0   | 0.81            | 0.89          |
| 14.1   | 0.81            | 0.89          |
| 15.9   | 0.88            | 1.11          |
| 16.0   | 0.88            | 1.08          |
| 18.0   | 0.92            | 1.03          |
| 20.0   | 0.98            | 1.17          |
| 20.1   | 0.98            | 1.41          |
| 25.0   | 1.10            | 1.41          |
| 25.0   | 1.10            | 1.29          |
| 25.0   | 1.10            | 1.56          |
| 30.2   | 1.21            | 1.92          |
| 35.0   | 1.30            | 1.83          |
| 39.4   | 1.36            | 2.08          |
| 39.4   | 1.36            | 2.20          |
| 44.5   | 1.46            | 1.92          |
| 45.6   | 1.48            | 2.10          |
| 49.4   | 1.54            | 2.16          |
| 55.2   | 1.63            | 1.90          |
| 59.8   | 1.70            | 2.13          |
| 65.1   | 1.77            | 1.83          |
| 69.3   | 1.83            | 1.98          |
| 75.2   | 1.90            | 1.75          |
| 79.7   | 1.96            | 1.77          |
| 85.2   | 2.03            | 1.58          |
| 90.1   | 2.08            | 1.59          |
| 95.3   | 2.14            | 1.59          |
| 99.7   | 2.19            | 1.70          |
|        | He atoms        |               |
| 10.0   | 0.69            | 0.37          |
| 12.0   | 0.75            | 0.75          |
| 14.0   | 0.81            | 0.88          |
| 16.0   | 0.88            | 0.78          |
| 16.1   | 0.88            | 0.82          |
| 18.0   | 0.92            | 0.85          |
| 20.0   | 0.98            | 1.04          |
| 20.1   | 0.98            | 1.13          |
| 25.0   | 1.10            | 1.23          |
| 25.0   | 1.10            | 1.21          |
| 29.9   | 1.2             | 1.31          |
| 30.0   | 1.2             | 1.32          |
| 31.5   | 1.23            | 1.51          |
| 35.0   | 1.30            | 1.59          |
| 39.3   | 1.38            | 2.02          |
| 45.0   | 1.47            | 2.05          |
| 49.2   | 1.54            | 2.41          |
| 55.2   | 1.63            | 2.48          |
| 59.4   | 1.69            | 2.91          |
| 64.8   | 1.77            | 2.72          |
| 69.3   | 1.83            | 3.06          |

TABLE II. (Continued)

| Energy | Velocity            | Cross section |
|--------|---------------------|---------------|
|        | He atoms            |               |
| 75.2   | 1.90                | 2.89          |
| 79.7   | 1.96                | 3.24          |
| 85.2   | 2.03                | 3.05          |
| 90.0   | 2.08                | 3.13          |
| 95.3   | 2.14                | 2.95          |
| 99.7   | 2.19                | 3.34          |
|        | He metastable atoms |               |
| 10.0   | 0.69                | 13.4          |
| 15.0   | 0.84                | 4.1           |
| 20.0   | 0.98                | 3.6           |
| 25.0   | 1.10                | 4.4           |
| 30.0   | 1.20                | 3.8           |
| 30.0   | 1.20                | 3.7           |
| 70.0   | 1.85                | 4.2           |

larger radius of its electronic orbits and/or the presence of two electrons instead of one. It is also possible that the net charge in the case of He<sup>+</sup> may have an influence.

A second comparison of interest is that of He<sup>+</sup> with H, where  $\Delta E$  is the same. It is noted that the He<sup>+</sup> cross section peaks at about  $1.5 \times 10^8$  cm/sec and that the H cross section, as expected, peaks at a somewhat lower velocity. However, the peak value of the H cross section is greater. The fact that the radius of the hydrogen atom is greater may be important. Also shown in Fig. 3 are the data for H and H<sup>+</sup> obtained by the Montana State University (MSU) group. It would appear strange that the two sets of 3371-Å cross sections show fairly good agreement in view of the discrepancy for the N<sub>2</sub><sup>+</sup> (3914-Å) data. The 3914-Å cross sections of the MSU group were normalized in the energy range from 40 to 70 keV to those of Philpot and Hughes,<sup>3</sup> whose values are about a factor of 1.5 greater than those reported here. While the MSU group corrected its data for the monochromator response in changing from 3914 to 3371 Å, it is our understanding<sup>13</sup> that no such correction was made for the change in photomultiplier response. For an S-20 photocathode and quartz optics, there is perhaps a 10% difference in quantum efficiencies, with the 3914-Å efficiency being greater. Had the correction been made, the MSU 3371-Å cross sections would have been greater than reported; however, there would still be a substantial unexplained discrepancy.

It is also of interest to compare ground-state He with metastable He. Although the data for He (2<sup>3</sup>S) are fragmentary and have a much greater uncertainty than the data for He (1<sup>1</sup>S), they do indicate a larger cross section, particularly at the lowest energies. The  $\Delta E$  for a case of this type is some-

what ambiguous since a number of different final He states are possible. This results in a  $\Delta E$  which ranges from 11.8 to 15.7 eV for the endothermic cases and about 9 eV (exothermic) for the ground state. If such a mixture of final states does occur, one might expect to find no well-defined maxima, and this seems to be the case. This rapid rise in the metastable cross section as the energy is decreased may be reflected in the behavior of the  $\text{He}^+$  and ground-state He cross sections. There appears to be a tendency for these cross sections to have considerable scatter and perhaps small local maxima at about  $7 \times 10^7$  cm/sec. We believe that each of these beams could contain a small admixture of He ( $2^3\text{S}$ ); thus the large cross section for the metastable component would cause an increase in the observed cross sections.

Some comments must be made regarding the cross section for  $\text{H}^+$ . We believe that our measurements are probably accurate within about 20% for velocity greater than  $2.8 \times 10^8$  cm/sec. Below that energy we encountered great difficulties because of electron capture in the region between the magnet and the reaction chamber. For example, at  $1.4 \times 10^8$  cm/sec, if only 2% of the  $\text{H}^+$  beam captures electrons in this region, the apparent emission cross section would be  $10^{-19}$  cm<sup>2</sup>. At this velocity and for our path length, a background  $\text{N}_2$  pressure of about  $5 \times 10^{-6}$  Torr would produce this apparent cross section without any direct contribution from the  $\text{H}^+$  beam. While in principle one can correct for this effect by examination of the signal at each pressure with the charged beam discarded, the corrections are so large as to render the result meaningless. The situation improves rapidly as the velocity is increased because the electron-capture cross section for  $\text{H}^+$  and the emission cross section for H atoms both decrease rapidly. We believe that the values at velocities below  $2.8 \times 10^8$  cm/sec, with the very large scatter in these values obtained by the MSU group,<sup>2</sup> probably came from such effects. We were able to obtain such values with less scatter until the contribution from the neutral component was taken into account. At present, we are only prepared to state that the  $\text{H}^+$  cross section at  $2.2 \times 10^8$  cm/sec is less than  $10^{-19}$  cm<sup>2</sup>. We conclude that the  $\text{H}^+$  cross section is generally very small and that it decreases rapidly as the velocity is decreased in the region below  $2.8 \times 10^8$  cm/sec.

It was noted in the Introduction that information could be obtained from the second-order pressure coefficient. The second-order processes in general are (i) charge changing of the primary projectile with the resultant change in signal which is proportional to the difference of the emission cross sections of the modified and original projectiles, and (ii) the production of free electrons which in

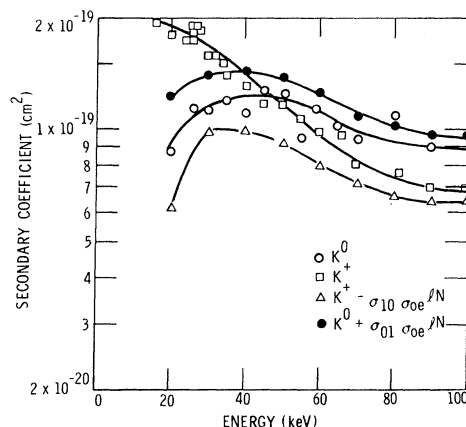


FIG. 6. Second-order coefficients  $K^+$  and  $K^0$  as a function of energy for incident  $\text{H}^+$  and H atoms, respectively. Also shown are coefficients corrected for charge-transfer effects where  $\sigma_{10}$  is the capture cross section for  $\text{H}^+$  in  $\text{N}_2$ ,  $\sigma_{01}$  is the stripping cross section for H atoms in  $\text{N}_2$ ,  $\sigma_{oe}$  is the emission cross section for H atoms,  $l$  is the effective chamber depth, in cm, to the observation region, and  $N$  is the number density of the target gas.

turn produce excitation in subsequent collisions.

Comparison of the second-order coefficients for  $\text{H}^+$  and H is of particular interest. Although the  $\text{H}^+$  cross sections have great uncertainty, as noted, the second-order coefficients may be measured with fair accuracy. Furthermore, each of these may be corrected for charge-transfer effects. In Fig. 6 we see that the corrected curves have the same shape, with the H curve significantly higher than the  $\text{H}^+$  curve. In principle, at least, we can associate this difference with the difference in excitation by free electrons. One cannot help noting in the stripping process,  $\text{H} + \text{N}_2 \rightarrow \text{H}^+ + \text{N}_2 + e$ , that the electron would have energy resulting from the projectile motion even if it is given no excess energy in the ionization process. For a 20-keV hydrogen atom, this results in an electron kinetic energy of about 10.8 eV, very close to the threshold for excitation of the  $\text{C}^3\Pi$  state. One would thus expect to find a substantial number of such electrons at energies near 14 eV, the peak of the cross section. Data are not presented for the second-order effects for He and  $\text{He}^+$ , since these are sufficiently small, relative to the first-order effects, that no valid results can be presented.

#### ACKNOWLEDGMENTS

The authors gratefully acknowledge the assistance of Laurence Ruggles and Orrin Smith in the acquisition of data. Our thanks are due also to M. A. Palmer for optical calibrations. Dr. Frank Biggs's advice in the analysis of the data was of considerable aid.

\*Work supported by the United States Atomic Energy Commission.

<sup>1</sup>E. W. Thomas, G. D. Bent, and J. L. Edwards, Phys. Rev. **165**, 32 (1968).

<sup>2</sup>D. A. Dahlberg, D. K. Anderson, and I. E. Dayton, Phys. Rev. **164**, 20 (1967).

<sup>3</sup>J. L. Philpot and R. H. Hughes, Phys. Rev. **133**, A107 (1964).

<sup>4</sup>M. Dufay, J. Desesquelles, M. Druetta, and M. Eidelsberg, Ann. Geophys. **22**, 614 (1966).

<sup>5</sup>J. M. Robinson and H. B. Gilbody, Proc. Phys. Soc. (London) **92**, 589 (1967).

<sup>6</sup>H. A. B. Gardiner, W. R. Pendleton, Jr., J. J. Merrill, and D. J. Baker, Phys. Rev. **188**, 257 (1969).

<sup>7</sup>F. J. DeHeer and J. F. M. Aarts, Physica **48**, 620 (1970).

<sup>8</sup>W. F. Sheridan, O. Oldenberg, and N. P. Carleton, J. Geophys. Res. **76**, 2429 (1971).

<sup>9</sup>D. J. Burns, F. R. Simpson, and J. W. McConkey, J. Phys. B **2**, 52 (1969) (also contains references to other measurements.)

<sup>10</sup>W. E. Lamb, Jr. and R. C. Retherford, Phys. Rev. **79**, 549 (1950).

<sup>11</sup>R. E. Miers, A. S. Schlachter, and L. W. Anderson, Phys. Rev. **183**, 213 (1969). [See also H. B. Gilbody, R. Browning, G. Levy, A. I. McIntosh, and K. F. Dunn, J. Phys. B **1**, 863 (1968).]

<sup>12</sup>J. M. Hoffman, G. J. Lockwood, and G. H. Miller, Sandia Laboratories Report No. SC-RR-70-695, 1970 (unpublished).

<sup>13</sup>D. K. Anderson (private communication).

## Total Cross Sections for Charge Transfer and Stripping of Al, Cr, and Er Ions in He and N<sub>2</sub><sup>†</sup>

Grant J. Lockwood

Sandia Laboratories, Albuquerque, New Mexico 87115

(Received 19 June 1972)

Absolute measurements are reported of the total cross sections for charge transfer and stripping of Er<sup>+</sup>, Er<sup>2+</sup>, Al<sup>+</sup>, and Cr<sup>+</sup> ions incident on He and N<sub>2</sub> in the energy range from 15 to 100 keV. These measurements include  $\sigma_{10}$ ,  $\sigma_{12}$ , and  $\sigma_{21}$ . The  $\sigma_{12}$  cross sections are greater than those of the  $\sigma_{10}$  at the same velocity for all ions except Cr<sup>+</sup>. Charge-transfer cross sections  $\sigma_{10}$  have a velocity dependence which is not predicted by the simple adiabatic criterion.

### I. INTRODUCTION

Cross sections for charge transfer and stripping of various ions in noble and atmospheric gases have been the subject of much research. However, most of the work has been carried out with ions of the noble and atmospheric gases and the alkali metals. Recently, this work has been expanded to ions of various metals. This report furthers this work in that it examines in detail the unexpected energy dependence, as reported by Layton *et al.*<sup>1</sup> of the total cross section for charge transfer  $\sigma_{10}$  for Al<sup>+</sup> in N<sub>2</sub> below 100 keV. In addition, it presents total cross sections involving ions of Al, Cr, and Er not previously reported. Cross sections which have been measured are listed in Table I.

These cross sections were measured as a function of energy from 15 to 100 keV with the exception of Er<sup>+</sup> which was limited to 70 keV by the accelerator analyzing magnet.

### II. APPARATUS AND EXPERIMENTAL PROCEDURES

The Sandia Laboratories 100-kV ion accelerator was used in this study. The Al<sup>+</sup> and Cr<sup>+</sup> ions were obtained from thermionic sources. The Al source was made by flame spraying Al<sub>2</sub>O<sub>3</sub> onto a tantalum filament; the Cr source was made by coating a tungsten filament with Cr<sub>2</sub>O<sub>3</sub> which had been mixed

with distilled water. When the filaments were heated in a vacuum, singly charged ions of the metal were emitted. This type of source gives ions in the ground state only. The Er<sup>+</sup> and Er<sup>2+</sup> ions were from a modified electron impact source in which a second filament containing Er metal was used. A discharge was maintained with Ar gas and the Er-coated filament heated to supply Er vapor. Since this source was energetic enough to supply both Er<sup>+</sup> and Er<sup>2+</sup>, the ion beams could have contained long-lived excited states as well as ground-state ions, provided that such states exist and have lifetimes greater than 10<sup>-5</sup> sec. This time is based on time of flight of the ions from source to experimental chamber at maximum energy. The accelerator delivers a beam of magnetically analyzed ions having small energy spread to the experimental chamber. Figure 1 shows the magnetically analyzed, singly ionized outputs of these

TABLE I. Measured cross sections.

| Ion              | Helium target               | Nitrogen target             |
|------------------|-----------------------------|-----------------------------|
| Al <sup>+</sup>  | $\sigma_{10}$ $\sigma_{12}$ | $\sigma_{10}$               |
| Cr <sup>+</sup>  | $\sigma_{10}$ $\sigma_{12}$ | $\sigma_{10}$               |
| Er <sup>+</sup>  | $\sigma_{10}$ $\sigma_{12}$ | $\sigma_{10}$ $\sigma_{12}$ |
| Er <sup>2+</sup> | $\sigma_{21}$               | $\sigma_{21}$               |